A Finite Element Analysis of Planar Circulators Using Arbitrarily Shaped Resonators

RONALD W. LYON, MEMBER, IEEE AND JOSEPH HELSZAJN, MEMBER, IEEE

Abstract—**A planar circulator consists, in general, of three transmission lines, connected through suitable matching networks to a magnetized ferrite resonator having three-fold symmetry. This paper describes a finite element analysis which enables the Z-matrix of a planar circulator using arbitrary shaped resonators to be calculated. This technique allows quite general computer programs to be written which permit tables of circulation solutions to be calculated. Results for junctions using disk, triangular, and irregular hexagonal resonators are included in the text. The frequency response of junction circulators using various configurations whose magnetic variables have been chosen so that they operate over the widely used tracking interval has also been evaluated. The optimum response is in each case associated with a unique coupling angle.**

I. Introduction

A PLANAR junction circulator consists, in general, of a three-fold symmetric resonator of arbitrary shape to which three transmission lines are connected. A complete description of planar circulators using disk resonators has been presented in the literature [1]–[5], and some approximate analyses are available for junctions using triangular [6] and Wye [7] resonators. The general boundary value problem has been treated by Miyoshi [8], [9] who used a contour integration formulation to form the entries of the impedance matrix of the junction. Miyoshi also presented an alternative analysis in which the open circuit parameters of the junction are expanded in terms of the modes of the magnetized planar resonator. The decoupled resonator is analyzed using a variational method where the fields are expressed as a single polynomial expansion for the complete resonator. This second method requires that a mathematical derivation of the polynomial coefficients be derived analytically for each individual resonator shape required.

This paper describes a finite element approach using the variational formulation introduced by Miyoshi. The method, which reduces to that of Silvester [10]–[14] in the demagnetized case, differs from that of Miyoshi in that it permits a complicated resonator shape to be subdivided into a number of smaller elements, thus allowing a quite general computer program to be written. Both the finite element method, described in this paper, and the contour integration method used by Miyoshi, currently require the manipulation of relatively large matrices. The finite element method, however, has the advantage that it is possible to build on the work which has been found valuable in waveguide analysis. The contour integration approach requires that the matrix problem be recomputed for each coupling width chosen, whereas in the finite-element approach the coupling angle is not chosen until after the matrix manipulations are completed. This may result in a computational saving if a large number of coupling angles are to be considered.

To determine the performance of the three-port device as a circulator, the circulation boundary conditions [3] are imposed on the elements of the Z matrix. This gives the operating frequency and gyrator level of the device and, subsequently, allows the frequency response to be calculated. Circulation conditions over the complete κ/μ range for circulators using disk, irregular hexagonal, and triangular resonators are presented in this paper. As an application of this work, the frequency response of the input admittance has been evaluated with $\kappa/\mu = 0.67$ at the center frequency.

It is shown that circulators using each resonator shape can be arranged to exhibit well-behaved equivalent circuits. These would be consistent with the design of an octave-band circulator subject to the design of a suitable matching network. None of the resonators analyzed, however, exhibit characteristics which would allow any one to be designated 'ideal' for the design of octave-band circulators.

II. Electromagnetic and Network Formulation for Planar Junction Circulators

One description of a planar junction circulator is in terms of its impedance matrix. In order to obtain this matrix, the relationship between the electric and magnetic fields at the coupling ports must be determined. Bosma [1], [2] has obtained such a relationship for a disk circulator using Green's function techniques. A similar procedure has been utilized by Miyoshi [8] for arbitrary resonator shapes in which he derives an expansion for the open circuit parameters in terms of a series of eigenfunctions ϕ_a which

Manuscript received August 18, 1981; revised May 19, 1982.

R. W. Lyon was with Heriot–Watt University, and is now with ERA Technology Ltd., Leatherhead, Surrey, England.

J. Helszajn is with Heriot–Watt University, Department of Electrical Engineering, 31–35 Grassmarket, Edinburgh, EH1 2HT, Scotland

0018-9480/82/1100-1964$00.75 ©1982 IEEE

he calculates using a variational method. In this section, this expansion due to Miyoshi is developed.

A generalized schematic diagram of a circulator is shown in Fig. 1. It consists of a three-fold symmetric, magnetized, ferrite resonator to which coupling lines are connected. These are printed onto either a dielectric or demagnetized ferrite substrate. The boundary of the resonator is designated by a contour ξ along which two unit vectors are defined, a normal vector $\hat{n}$ and a tangential vector $\hat{t}$. The separation H between the ground plane and the center conductor is arranged to be small with respect to the wavelength in order to ensure that higher order modes which vary in the z direction are suppressed. This restriction, when applied together with the boundary conditions on the center conductor, implies that only the (E_z, H_x, H_y) field components exist.

The E_z field in a planar junction circulator satisfies the wave equation [1], [2]

$$\left(\nabla_t^2 + k_{\text{eff}}^2\right) E_z = 0 \tag{1}$$

where k_{eff}, the wave number, is given by

$$k_{\text{eff}}^2 = \omega^2 \mu_0 \mu_{\text{eff}} \epsilon_0 \epsilon_f. \tag{2}$$

ϵ_f is the relative permittivity of the ferrite medium, and the effective permeability μ_{eff} is given by

$$\mu_{\text{eff}} = \frac{\mu^2 - \kappa^2}{\mu} \tag{3}$$

where μ and κ are the diagonal and off-diagonal components of the tensor permeability of the ferrite.

On the boundary, the tangential magnetic field H_t is equal to zero and this may be expressed as a boundary condition on E_z to give

$$\frac{\partial E_z}{\partial n} + j\frac{\kappa}{\mu}\frac{\partial E_z}{\partial t} = 0 \qquad \text{on } \xi. \tag{4a}$$

At the coupling ports, H_t is not zero and E_z satisfies

$$\frac{\partial E_z}{\partial n} + j\frac{\kappa}{\mu}\frac{\partial E_z}{\partial t} = j\omega\mu_0\mu_{\text{eff}} H_t. \tag{4b}$$

In order to solve (1) in conjunction with (4a–b), it is convenient to introduce a Green's function $G(\boldsymbol{r}|\boldsymbol{r}_0)$. Two variables are defined when using a Green's function; the point $\boldsymbol{r}$ at which the E_z field is observed and the coupling port coordinate $\boldsymbol{r}_0$. These conventions are summarized in Fig. 2.

The Green's function $G(\boldsymbol{r}|\boldsymbol{r}_0)$ is defined as the solution to the equation

$$\left(\nabla_t^2 + k_{\text{eff}}^2\right) G(\boldsymbol{r}|\boldsymbol{r}_0) = -j\omega\mu_0\mu_{\text{eff}}\delta(\boldsymbol{r} - \boldsymbol{r}_0) \tag{5}$$

where $\delta(\boldsymbol{r} - \boldsymbol{r}_0)$ is the dirac delta function. The Green's function must satisfy the boundary condition

$$\frac{\partial G(\boldsymbol{r}|\boldsymbol{r}_0)}{\partial n} - j\frac{\kappa}{\mu}\frac{\partial G(\boldsymbol{r}|\boldsymbol{r}_0)}{\partial t} = 0. \tag{6}$$

The Green's function, whose units are (Ω/m), is a generalization of that used for a disk by Bosma [1] who sets

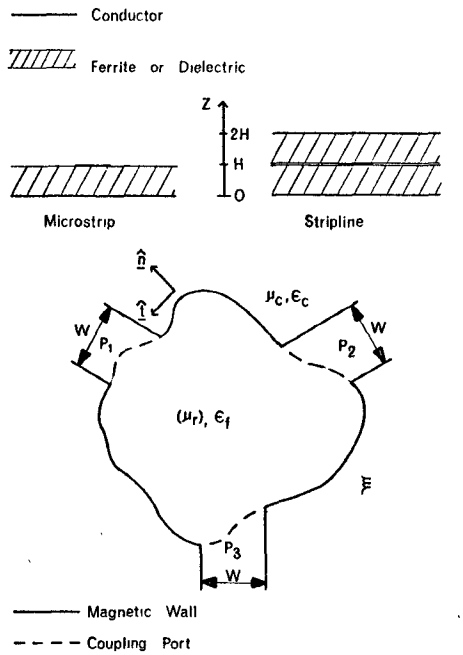

Fig. 1. Generalized schematic diagram of planar junction circulator.

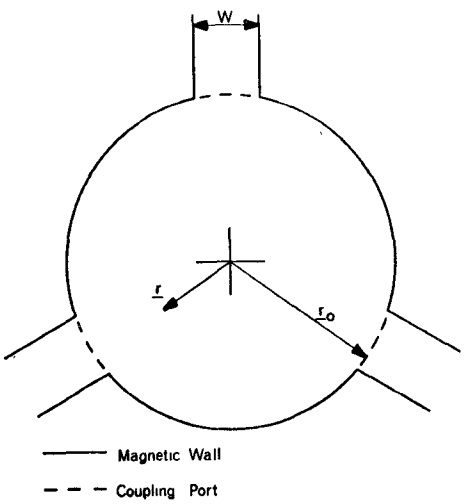

Fig. 2. Coordinate convention for Green's function.

out its properties in detail and show that

$$E_z(\boldsymbol{r}) = \sum_{i=1}^{3} \int_{P_i} G(\boldsymbol{r}|\boldsymbol{r}_0) H_t(\boldsymbol{r}_0)\, dt_0 \tag{7}$$

where the integration is carried out over the coupling port P_i. $E_z(\boldsymbol{r})$ applies at any point in the resonator including the intervals defined by the coupling points.

At this point, the derivation of Miyoshi's [8] contour integration method and variational method diverge. The contour integration method consists of discretizing the boundary and, by employing a different Green's function which satisfies the wave equation but which does not satisfy (6), reducing a contour integration whose form is similar to (7) to a set of matrix equations. In his variational approach, Miyoshi expanded the Green's function as a

series of eigenfunctions ϕ_a to give

$$G(\boldsymbol{r}|\boldsymbol{r}_0) = j\omega\mu_0\mu_{\text{eff}} \sum_{a=1}^{\infty} \frac{\phi_a(\boldsymbol{r})\phi_a^*(\boldsymbol{r}_0)}{k_a^2 - k_{\text{eff}}^2}. \tag{8}$$

In practice, sufficiently accurate results are obtained when this series is truncated to around 10 terms. The eigenfunctions ϕ_a and the eigenvalues k_a are the solutions to the differential equation

$$\left(\nabla_t^2 + k_a^2\right)\phi_a(\boldsymbol{r}) = 0 \tag{9}$$

subject to the boundary condition imposed on the Green's function given in (6). The eigenfunctions are orthogonal and are normalized so that

$$\int\int_s \phi_a(\boldsymbol{r})\phi_a^*(\boldsymbol{r})\, ds = 1. \tag{10}$$

In the demagnetized planar circuit, ϕ_a is directly equivalent to the electric field of the resonant modes in the planar resonator, whereas, in the magnetized case, ϕ_a represents the complex conjugate of E_z.

Assuming that H_t is a constant over each coupling port, Miyoshi derived the relation between the average electric field at port i and the magnetic field at port j from (7) and (8) giving

$$\eta_{ij} = \frac{j\omega\mu_0\mu_{\text{eff}}}{W} \sum_{a=1}^{\infty} \frac{1}{k_a^2 - k_{\text{eff}}^2} \int_{P_i} \phi_a^*(\boldsymbol{r})\, dt \int_{P_j} \phi_a(\boldsymbol{r}_0)\, dt_0 \tag{11}$$

assuming all ports other than j are open circuited.

In order to derive a relationship for Z_{ij} from (11) it is necessary to introduce the characteristic impedance R_e of a planar transmission line of width W, substrate thickness H, and constitutive parameters ε_f and μ_{eff}. In stripline, R_e may be calculated using Richardson's technique [15] while the equivalent waveguide technique is commonly used in microstrip [17], [18]. For an n port where each of the coupling ports are of equal width W, Z_{ij} is given by

$$Z_{ij} = \frac{jR_e k_{\text{eff}}}{W} \sum_{a=1}^{\infty} \frac{1}{k_a^2 - k_{\text{eff}}^2} \int_{P_i} \phi_a^*(\boldsymbol{r})\, dt \int_{P_j} \phi_a(\boldsymbol{r})_0\, dt_0. \tag{12}$$

This analysis is a more general statement of the treatment presented by Bosma [2] for the particular case of a disk resonator.

III. Variational Solution for Eigenfunctions Using Matrix Eigenvalue Method

The Z matrix of a junction circulator can be derived provided that the eigenfunctions ϕ_a, which satisfy (9) together with the boundary conditions given by (6), are known. It is only possible to solve these equations analytically in a very small number of cases, and the most convenient method, in the general case, is to use a variational approach.

Miyoshi [8] has recognized that the trial function ϕ_a', which causes the functional

$$F(\phi_a'(\boldsymbol{r})) = \int\int_s |\nabla_t \phi_a'(\boldsymbol{r})|^2 - k_a^2 |\phi_a'(\boldsymbol{r})|^2\, ds - j\frac{\kappa}{\mu} \oint_\xi (\phi_a'(\boldsymbol{r}))^* \frac{\partial \phi'(\boldsymbol{r})}{\partial t}\, dt \tag{13}$$

to be minimized, satisfies both the differential equation and the boundary conditions for the eigenfunctions ϕ_a. When the value of κ/μ is set to zero, $F(\phi_a')$ reduces to the functional used by Silvester [10] in his analysis of arbitrarily shaped waveguides.

The trial function ϕ_a' is an approximation to the exact function ϕ_a and it is expanded as

$$\phi_a'(\boldsymbol{r}) = \sum_{i=1}^{n} u_i \alpha_i. \tag{14}$$

The terms α_i are a suitable set of real basis functions and u_i are the complex coefficients. There are n basis functions included in the expansion. In this paper, the basis functions are chosen using the finite element method.

Substituting (14) into the functional $F(\phi_a')$ in (13) and ensuring that the functional is minimized by imposing the Rayleigh–Ritz condition

$$\frac{\partial F(\phi_a'(\boldsymbol{r}))}{\partial u_i^*} \tag{15}$$

reduces the problem to a set of simultaneous equations of the form

$$[[A] - k_a^2[B]][u] = 0 \tag{16}$$

which may be recognized to be the general matrix eigenvalue problem

$$[A][u] = k_a^2[B][u]. \tag{17}$$

If the symmetric square matrix B is reduced to the product LL^T, where L is a lower triangular matrix, (17) may be reduced to the familiar eigenvalue problem

$$[L^{-1}][A][L^{-1}]^T[u] = k_a^2[u]. \tag{18}$$

A and B are square matrices

$$A_{ij} = \int\int_s \nabla_t \alpha_i \cdot \nabla_t \alpha_j\, ds - j\frac{\kappa}{\mu} \oint_\xi \alpha_i \frac{\partial \alpha_j}{\partial t}\, dt \tag{19}$$

and may be reduced to

$$[A] = [D] + j\frac{\kappa}{\mu}[C] \tag{20}$$

where

$$D_{ij} = \int\int_s \nabla_t \alpha_i \cdot \nabla_t \alpha_j\, ds \tag{21a}$$

$$C_{ij} = -\oint_\xi \alpha_i \frac{\partial \alpha_j}{\partial t}\, dt. \tag{21b}$$

The elements of the B matrix are given by

$$B_{ij} = \int\int_s \alpha_i \alpha_j\, ds. \tag{22}$$

The B matrix is reduced to LL^T computationally and, thus,

an analytic expression for L is not given. Once n is selected, the matrix eigenvalue equation will yield n eigenvalues k_a^2 and column eigenvectors $[u]$, n is the number of basis functions included in (14).

Silvester, using the finite element method, has calculated both the B matrix and the D matrix (the B matrix is the T matrix and the D matrix is the S matrix in Silvester's notation) which are symmetric and are fully tabulated in [11]. The C matrix is skew-symmetric and is derived in this paper.

IV. Finite Element Analysis

In the variational method, it is possible to choose any suitable set of basis functions to expand the trial function ((14)). Miyoshi [8] uses a polynomial expansion which describes the fields in the complete resonator. This has the disadvantage that the A and B matrices given by (20) and (22) must be recalculated for every different resonator shape. In the finite element method used by Silvester [10]–[14] in his analysis of arbitrary shaped waveguides, this problem is overcome by subdividing the resonator region into triangular elements. A polynomial expansion for the eigenfunction ϕ_a is formed in each triangle in terms of $(u_i\alpha_i)$ in (14) enabling the A and B matrices to be calculated. These are then assembled together to form the complete matrix eigenvalue problem.

Using the finite element method, Silvester [11] has presented expressions for polynomial basis functions in triangular elements. These are given in terms of triangular area coordinates for each point inside a triangle. Each coordinates is defined as the ratio of the perpendicular distance to the wall opposite vertex i to the length of the altitude drawn to vertex i. From Fig. 3 it can be seen that the α_1 coordinate of point Q is given by

$$\zeta_1 = \frac{e}{d} \tag{23}$$

and the other coordinates ζ_2 and ζ_3 are defined in a similar manner. It is important to note that the three coordinates are related by [11]

$$\zeta_1 + \zeta_2 + \zeta_3 = 1. \tag{24}$$

In the finite element method described in this paper, the basis functions α_i in (14) are polynomials of degree p and these are arranged to provide a p'th-order interpolation to the eigenfunction ϕ_a over each triangle. In general, a polynomial of degree p in two coordinates will have m coefficients where

$$m = (p+1)(p+2)/2. \tag{25}$$

Over each triangular element, m points (nodes) are distributed and each basis function is arranged to take the value 1 at one node and 0 at all the others. Thus, the coefficients of the basis functions α_i in (14) represent the amplitude of the eigenfunction ϕ_a' at point i. The distribution of the nodes over a triangle for first-, second-, third-, and fourth-order polynomials are illustrated in Fig. 4. Each point is labeled with three integers, i, j, and k from which its triangular area coordinates $(\zeta_1, \zeta_2, \zeta_3)$ can be

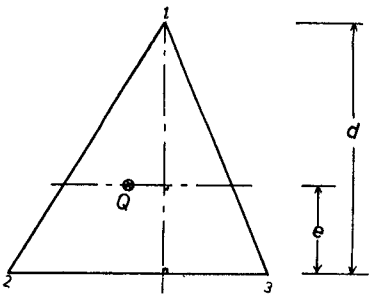

Fig. 3. Dimensions used in the definition of triangular area coordinates.

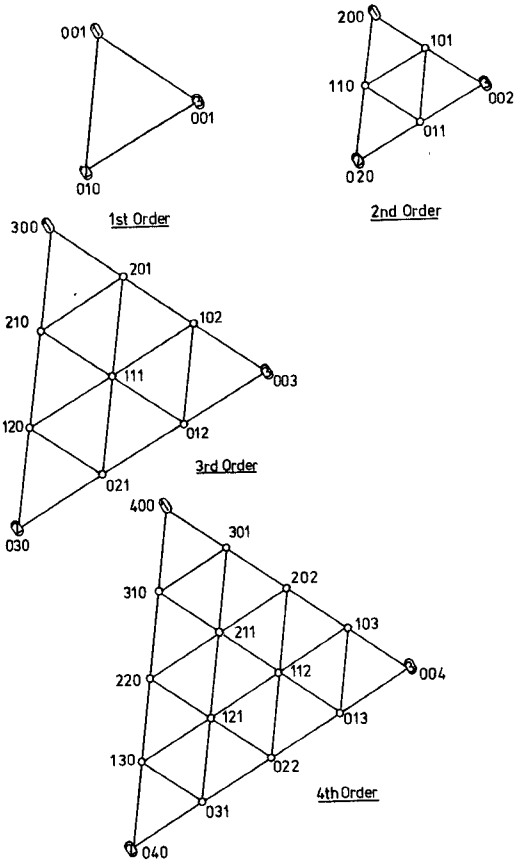

Fig. 4. Distribution of nodes over triangle for first-, second-, third-, and fourth-order polynomials.

derived using the relation

$$(\zeta_1, \zeta_2, \zeta_3) = \left(\frac{i}{p}, \frac{j}{p}, \frac{k}{p}\right). \tag{26}$$

Equation (24) is also satisfied since

$$i + j + k = p. \tag{27}$$

Associated with each point is a basis function $\alpha_{ijk}(\zeta_1, \zeta_2, \zeta_3)$ which is given by [11]

$$\alpha_{ijk}(\zeta_1, \zeta_2, \zeta_3) = P_i(\zeta_1) P_j(\zeta_2) P_k(\zeta_3) \tag{28}$$

where

$$P_r(\zeta_q) = \prod_{L=1}^{r} \left(\frac{P(\zeta_q) - L + 1}{L}\right), \qquad r \geq 1 \tag{29a}$$

$$= 1, \qquad r = 0 \tag{29b}$$

where q and r are dummy variables which satisfy $q \in \{1, 2, 3\}$

and $r \in \{i, j, k\}$. The basis function α_{ijk} takes the value 1 at node (i, j, k) and the value 0 at all other nodes in the triangle.

These formulas may now be substituted into (20) and (22) to calculate the A and B matrices for a triangle.

The number of terms taken in (14) is determined by the number of triangles included in a finite element division of any particular resonator shape. There is not a simple relation between the number of elements and the number of basis functions since, in essence, there will be one basis function for each node in the resonator. The number of nodes in a particular element is a function of the order of the polynomial approximation within that element. Equation (25) gives the number of nodes in each element as a function of the nodes of approximation p.

In addition to the order of polynomial approximation within each element the total number of nodes in any resonator is determined by the number and orientation of the elements in the resonator. This is demonstrated in Fig. 5, in which a triangle is split into three elements each of which, individually, have three nodes. Once they are assembled, however, certain nodes coincide leaving only four in total. Thus, it is not possible to make a simple statement of the value of n in (14). In practice, the value $90 < n < 100$ have been found to give accurate results.

The C matrix involves integration around the contour ξ and so the matrix has the value [0] if the element does not lie along the boundary. If the element has one or more of its sides lying along the boundary the C matrix for this element can be written down provided it is known for the case where an element has only one side on the boundary.

Consider the case where the first-order polynomial interpolation is to be employed (i.e., $p = 1$ in (25)). The following expressions for the basis functions $\alpha_{100}, \alpha_{010}$, and α_{001} can be derived from (28):

$$\begin{aligned} \alpha_{100} &= \zeta_1 \\ \alpha_{010} &= \zeta_2 \\ \alpha_{001} &= \zeta_3. \end{aligned} \tag{30}$$

Substituting these expressions into (21b) leads to the following expression for the C matrix when the magnetic wall lies opposite the point (1,0,0):

$$[C^{(1,0,0)}] = \begin{bmatrix} 0 & 0 & 0 \\ 0 & 1 & -1 \\ 0 & 1 & -1 \end{bmatrix}. \tag{31}$$

This matrix can be seen to be skew symmetric.

If the boundary lies opposite points (0,1,0) or (0,0,1), the C matrix may be calculated simply by re-arranging the matrix derived for a boundary opposite (1,0,0). For example, in the case where a boundary lies opposite point (0,1,0), subscript (1) → (2) subscript (2) → (3), and subscript (3) → (1). Thus, the C matrix is given by

$$[C^{(0,1,0)}] = \begin{bmatrix} -1 & 0 & 1 \\ 0 & 0 & 0 \\ -1 & 0 & 1 \end{bmatrix}. \tag{32}$$

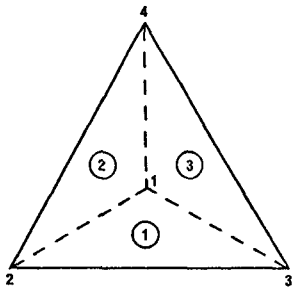

Fig. 5. Triangle split into three elements.

If the element has two of three sides which lie along the boundary, the C matrix is calculated by adding the matrices derived for elements which have magnetic walls on a single side.

The matrices given in (31) and (32) refer to a single, isolated triangular element. Several matrices must be assembled together, however, to form the complete eigenvalue problem. Consider the case illustrated in Fig. 5 where a triangle is split up into three elements in a fashion which preserves the 120° symmetry. The C matrix for the complete shape is given by

$$\begin{aligned} [C_4] &= \begin{bmatrix} 0 & 0 & 0 & 0 \\ 0 & 1 & -1 & 0 \\ 0 & 1 & -1 & 0 \\ 0 & 0 & 0 & 0 \end{bmatrix} + \begin{bmatrix} 0 & 0 & 0 & 0 \\ 0 & 0 & 0 & 0 \\ 0 & 0 & 1 & -1 \\ 0 & 0 & 1 & -1 \end{bmatrix} \\ &\quad + \begin{bmatrix} 0 & 0 & 0 & 0 \\ 0 & -1 & 0 & 1 \\ 0 & 0 & 0 & 0 \\ 0 & -1 & 0 & 1 \end{bmatrix} = \begin{bmatrix} 0 & 0 & 0 & 0 \\ 0 & 0 & -1 & 1 \\ 0 & 1 & 0 & -1 \\ 0 & -1 & 1 & 0 \end{bmatrix} \end{aligned} \tag{33}$$

which is also skew-symmetric. In the examples considered in this paper, the A, B, and C matrices, when finally assembled are of the order 100×100.

The calculation of the C matrix for first-order polynomials is reasonably easy, but for higher order polynomials the volume of algebra becomes too large to be performed by hand. Silvester [11] encountered similar difficulties and in order to overcome the problem a computer program was written to evaluate the matrix elements analytically. By adopting a similar approach the authors have evaluated the C matrices for up to fourth-order interpolation and these are tabulated in Table I. In most cases, fourth-order interpolation is the maximum which can be used in practice as there are 15 nodes in each element and large matrices can be generated when only a few elements are incorporated. Silvester [11] presents a table contrasting the relative merits of using higher order interpolation or alternatively more elements using a lower order polynomial approximation.

V. Computation of Circulation Conditions

A suite of computer programs have been written which implement the theoretical results discussed in the previous sections. These consist, firstly, of a program which uses the finite element method to evaluate the resonant modes of a

TABLE I
TABLE OF C MATRICES FOR POLYNOMIALS UP TO FOURTH ORDER

```
N= 1
COMMON DENOMINATOR IS    2

   0    0    0
   0    1   -1
   0    1   -1
```

```
N= 3
COMMON DENOMINATOR IS    80

   0    0    0    0    0    0    0    0    0    0
   0    0    0    0    0    0    0    0    0    0
   0    0    0    0    0    0    0    0    0    0
   0    0    0    0    0    0    0    0    0    0
   0    0    0    0    0    0    0    0    0    0
   0    0    0    0    0    0    0    0    0    0
   0    0    0    0    0    0   40  -57   24   -7
   0    0    0    0    0    0   57    0  -81   24
   0    0    0    0    0    0  -24   81    0  -57
   0    0    0    0    0    0    7  -24   57  -40
```

```
N= 2
COMMON DENOMINATOR IS    6

   0    0    0    0    0    0
   0    0    0    0    0    0
   0    0    0    0    0    0
   0    0    0    3   -4    1
   0    0    0    4    0   -4
   0    0    0   -1    4   -3
```

```
N= 4
COMMON DENOMINATOR IS 1890

   0    0    0    0    0    0    0    0    0    0    0    0    0    0    0
   0    0    0    0    0    0    0    0    0    0    0    0    0    0    0
   0    0    0    0    0    0    0    0    0    0    0    0    0    0    0
   0    0    0    0    0    0    0    0    0    0    0    0    0    0    0
   0    0    0    0    0    0    0    0    0    0    0    0    0    0    0
   0    0    0    0    0    0    0    0    0    0    0    0    0    0    0
   0    0    0    0    0    0    0    0    0    0    0    0    0    0    0
   0    0    0    0    0    0    0    0    0    0    0    0    0    0    0
   0    0    0    0    0    0    0    0    0    0    0    0    0    0    0
   0    0    0    0    0    0    0    0    0    0    0    0    0    0    0
   0    0    0    0    0    0    0    0    0    0  945-1472  804 -384  107
   0    0    0    0    0    0    0    0    0    0 1472    0-2112 1024 -384
   0    0    0    0    0    0    0    0    0    0 -804 2112    0-2112  804
   0    0    0    0    0    0    0    0    0    0  384-1024 2112    0-1472
   0    0    0    0    0    0    0    0    0    0 -107  384 -804 1472 -945
```

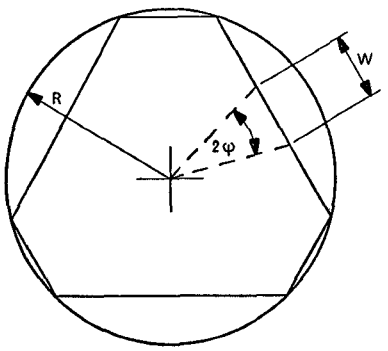

Fig. 6. Definition of coupling angle ψ.

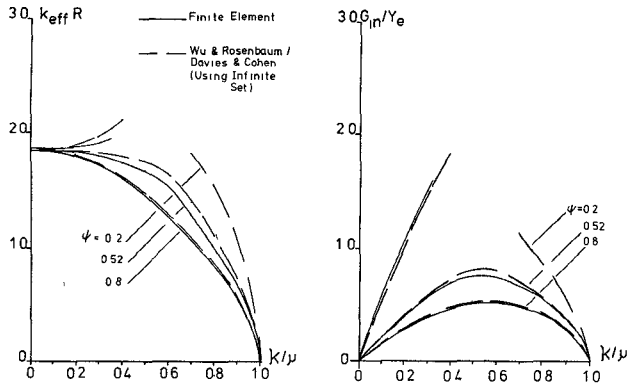

Fig. 7. Comparison between finite element and closed form (Davies and Cohen) solutions for disk resonator.

magnetized ferrite-loaded planar resonator. These resonant modes are then used by a second program to calculate the elements of the impedance matrix. This program then determines the lowest value of $k_{\mathrm{eff}}R$ which satisfies the first circulation condition [3].

$$\operatorname{Im}(Z_{\mathrm{in}})=0 \tag{34}$$

for a range of values of κ/μ and coupling angles (the angle which sustends the coupling interval W in Fig. 6). The input resistance of the circulator at this value of $k_{\mathrm{eff}}R$ is then calculated using the second circulation condition

$$R_{\mathrm{in}}=\operatorname{Re}(Z_{\mathrm{in}}) \tag{35}$$

where

$$Z_{\mathrm{in}}=Z_{11}+\frac{Z_{12}^2}{Z_{12}^*}. \tag{36}$$

In keeping with convention, the circulation data are tabulated in terms of G_{in} and B_{in} where

$$Y_{\mathrm{in}}=G_{\mathrm{in}}+jB_{\mathrm{in}}=\frac{1}{Z_{\mathrm{in}}}. \tag{37}$$

In Fig. 7(a) and (b), the results obtained using the method described in this paper are compared with those produced by previous authors for a disk [3], [5]. In calculating these results, the infinite series in (12) has been truncated to 10 terms. It can be seen that the agreement is best for larger coupling angles and less good for small values of ψ. The reason for this is that smaller coupling angles excite higher order modes more strongly, and these higher order modes tend to be computed less accurately by the finite element program.

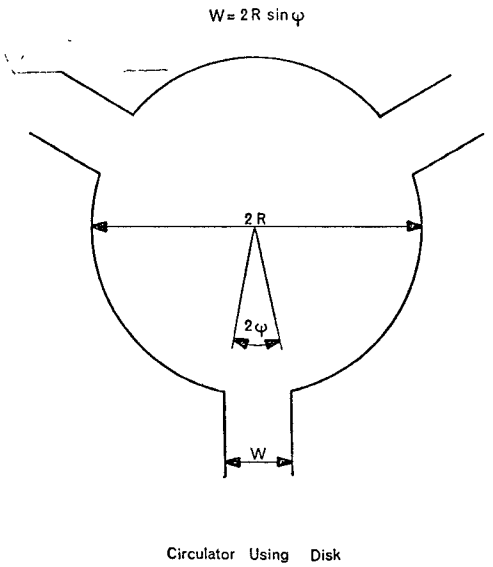

Fig. 8. Coordinate system of disk resonator.

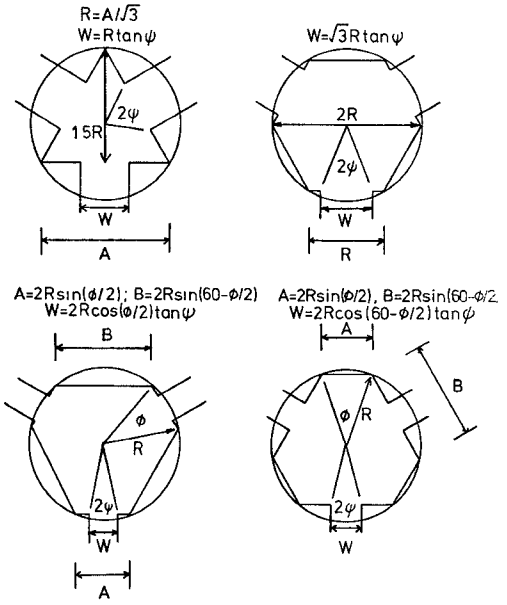

Fig. 9. Coordinate system of triangle, regular hexagonal, narrow, and broad-wall coupled irregular hexagonal resonators.

In Tables II–VI, the first and second circulation solutions are tabulated for disk, triangular, regular hexagon, narrow and broad wall coupled irregular hexagons illustrated in Figs. 8 and 9. These tables are computed retaining the first 10 eigenfunctions ϕ_a in (12). It is observed that at certain points in the tables (e.g., a triangle $0.7 < \kappa/\mu < 0.85$) the values $k_{\text{eff}}R$ and G_{in}/Y_f take the value 0. This indicates that no circulation condition was located with $k_{\text{eff}}R < 3.0$. In certain cases, G_{in}/Y_f takes a negative value. At these points, the lowest circulation condition represents rotation in the opposite direction.

The values of G_{in} and B_{in} are normalized to Y_f which is given by

$$Y_f = \sqrt{\epsilon_f}\, Y_r. \tag{38}$$

TABLE II
TABLES OF $k_{\text{eff}}R$ (TABLE A) AND G/Y_f (TABLE B) FOR CIRCULATORS USING DISK, TRIANGLE REGULAR HEXAGON, NARROW AND BROAD-WALL COUPLED IRREGULAR HEXAGON ($\phi = 50$), RESPECTIVELY

First circulation solution for disk circulator

PSI	0.200	0.300	0.400	0.500	0.600	0.700	0.800
K/U	Keff.R	Keff.R	Keff.R	Keff.R	Keff.R	Keff.R	Keff.R
0.10	1.862	1.859	1.857	1.854	1.851	1.848	1.846
0.15	1.864	1.859	1.852	1.845	1.839	1.833	1.828
0.20	1.869	1.859	1.847	1.834	1.821	1.810	1.801
0.25	1.880	1.861	1.840	1.818	1.798	1.780	1.766
0.30	1.903	1.869	1.833	1.798	1.767	1.741	1.720
0.35	1.968	1.889	1.826	1.772	1.729	1.693	1.665
0.40	2.206	1.968	1.823	1.741	1.681	1.636	1.600
0.45	2.216	2.180	1.842	1.711	1.630	1.572	1.529
0.50	2.228	2.224	2.192	1.664	1.564	1.497	1.448
0.55	0.000	0.000	0.000	1.605	1.487	1.414	1.361
0.60	2.193	2.187	2.171	1.532	1.402	1.325	1.270
0.65	2.162	2.136	2.071	1.443	1.308	1.230	1.175
0.70	2.518	2.064	1.884	1.305	1.204	1.133	1.078
0.75	2.342	1.941	1.692	1.190	1.088	1.023	0.972
0.80	2.328	1.762	1.469	1.068	0.969	0.907	0.859
0.85	2.375	1.519	1.235	0.927	0.836	0.779	0.736
0.90	1.973	1.214	0.976	0.756	0.679	0.631	0.594
0.95	0.904	0.812	0.654	0.530	0.477	0.442	0.415

Second circulation solution for disk circulator

PSI	0.200	0.300	0.400	0.500	0.600	0.700	0.800
K/U	Gin/Yf	Gin/Yf	Gin/Yf	Gin/Yf	Gin/Yf	Gin/Yf	Gin/Yf
0.10	0.495	0.335	0.255	0.210	0.181	0.162	0.149
0.15	0.750	0.505	0.383	0.314	0.271	0.242	0.223
0.20	1.010	0.676	0.511	0.417	0.359	0.320	0.295
0.25	1.282	0.850	0.637	0.517	0.443	0.394	0.363
0.30	1.580	1.029	0.760	0.612	0.522	0.463	0.427
0.35	1.980	1.223	0.882	0.701	0.593	0.526	0.484
0.40	3.011	1.500	1.001	0.780	0.656	0.580	0.534
0.45	2.685	1.728	1.079	0.837	0.706	0.623	0.572
0.50	2.828	1.803	1.350	0.893	0.749	0.660	0.606
0.55	-0.000	-0.000	-0.000	0.935	0.782	0.689	0.633
0.60	3.073	1.775	1.282	0.963	0.806	0.712	0.654
0.65	3.511	1.721	1.225	0.979	0.823	0.728	0.670
0.70	0.830	1.688	1.234	0.969	0.833	0.745	0.687
0.75	0.234	1.474	1.177	0.971	0.834	0.749	0.694
0.80	-0.429	1.356	1.154	0.972	0.839	0.755	0.700
0.85	-0.278	1.279	1.135	0.968	0.840	0.758	0.704
0.90	1.320	1.240	1.119	0.961	0.838	0.758	0.706
0.95	1.651	1.244	1.109	0.950	0.833	0.755	0.707

Y_r is the admittance of an air spaced planar transmission line whose width is defined by the coupling interval.

VI. Computation of Frequency Response

In addition to the calculation of circulation conditions, it is also necessary to investigate the frequency response of the input admittance of the junction. This is determined by a third program which evaluates the input admittance as a function of the normalized frequency variable

$$\delta = \frac{f - f_0}{f_0} \tag{39}$$

TABLE III
TABLES OF $k_{eff}R$ (TABLE A) AND G/Y_f (TABLE B) FOR CIRCULATORS USING DISK, TRIANGLE, REGULAR HEXAGON, NARROW AND BROAD-WALL COUPLED IRREGULAR HEXAGON ($\phi = 50$), RESPECTIVELY

First circulation solution for triangular circulator

PSI	0.200	0.300	0.400	0.500	0.600	0.700	0.800
K/U	Keff.R	Keff.R	Keff.R	Keff.R	Keff.R	Keff.R	Keff.R
0.10	2.455	2.450	2.444	2.438	2.432	2.428	2.426
0.15	2.451	2.438	2.423	2.409	2.396	2.397	2.382
0.20	2.448	2.421	2.392	2.366	2.346	2.331	2.323
0.25	2.458	2.402	2.351	2.312	2.283	2.262	2.250
0.30	2.504	2.386	2.301	2.247	2.210	2.183	2.166
0.35	2.536	2.383	2.241	2.174	2.127	2.089	2.061
0.40	2.524	2.518	2.175	2.095	2.040	1.996	1.961
0.45	2.493	2.492	2.101	2.007	1.946	1.897	1.857
0.50	2.448	2.445	2.021	1.916	1.849	1.795	1.751
0.55	1.993	1.910	1.845	1.790	1.743	1.703	1.671
0.60	1.990	1.837	1.756	1.691	1.638	1.593	1.557
0.65	2.263	1.767	1.662	1.586	1.525	1.475	1.431
0.70	0.000	1.703	1.559	1.473	1.407	1.353	1.305
0.75	0.000	2.042	1.444	1.352	1.284	1.230	1.182
0.80	0.000	0.000	1.309	1.209	1.142	1.090	1.046
0.85	0.000	0.000	1.154	1.054	0.990	0.941	0.900
0.90	2.690	2.508	0.948	0.861	0.808	0.766	0.731
0.95	0.631	0.634	0.865	0.931	0.583	0.547	0.518

Second circulation solution for triangular circulator

PSI	0.200	0.300	0.400	0.500	0.600	0.700	0.800
K/U	Gin/Yf	Gin/Yf	Gin/Yf	Gin/Yf	Gin/Yf	Gin/Yf	Gin/Yf
0.10	1.706	1.095	0.780	0.583	0.448	0.347	0.268
0.15	2.562	1.629	1.146	0.849	0.649	0.503	0.391
0.20	3.444	2.144	1.476	1.079	0.820	0.637	0.500
0.25	4.431	2.640	1.755	1.262	0.956	0.745	0.590
0.30	5.703	3.142	1.974	1.398	1.057	0.829	0.663
0.35	7.066	3.797	2.134	1.497	1.143	0.916	0.754
0.40	7.323	5.322	2.243	1.566	1.200	0.969	0.804
0.45	-21.798	5.174	2.310	1.604	1.236	1.004	0.841
0.50	7.199	4.965	2.348	1.629	1.262	1.033	0.870
0.55	4.847	2.835	1.960	1.489	1.197	0.993	0.836
0.60	5.556	2.915	1.998	1.518	1.222	1.016	0.861
0.65	10.533	2.979	2.014	1.535	1.242	1.042	0.893
0.70	-0.000	3.130	2.025	1.542	1.253	1.057	0.913
0.75	-0.000	5.718	2.029	1.537	1.251	1.059	0.917
0.80	-0.000	-0.000	2.067	1.556	1.265	1.069	0.925
0.85	-0.000	-0.000	2.052	1.540	1.255	1.064	0.923
0.90	1.454	1.031	1.996	1.501	1.230	1.048	0.913
0.95	3.585	2.438	2.765	2.541	1.249	1.054	0.915

TABLE IV
TABLES OF $k_{eff}R$ (TABLE A) AND G/Y_f (TABLE B) FOR CIRCULATORS USING DISK, TRIANGLE, REGULAR HEXAGON, NARROW AND BROAD-WALL COUPLED IRREGULAR HEXAGON ($\phi = 50$), RESPECTIVELY

First circulation solution using regular hexagon

PSI	0.200	0.300	0.400	0.500	0.524
K/U	Keff.R	Keff.R	Keff.R	Keff.R	Keff.R
0.10	2.004	2.003	2.002	2.000	1.999
0.15	1.997	1.994	1.990	1.985	1.984
0.20	1.985	1.981	1.974	1.965	1.963
0.25	1.973	1.965	1.953	1.938	1.934
0.30	1.960	1.946	1.928	1.905	1.899
0.35	1.945	1.924	1.896	1.863	1.856
0.40	1.930	1.897	1.857	1.813	1.803
0.45	1.917	1.866	1.811	1.754	1.742
0.50	1.913	1.829	1.755	1.686	1.671
0.55	0.000	1.783	1.688	1.608	1.592
0.60	2.348	1.726	1.610	1.522	1.504
0.65	2.267	1.653	1.519	1.426	1.407
0.70	2.151	1.551	1.413	1.321	1.302
0.75	2.012	1.854	1.276	1.184	1.174
0.80	1.849	1.691	1.166	1.064	1.051
0.85	1.660	1.484	1.028	0.928	0.914
0.90	1.464	1.218	0.838	0.764	0.753
0.95	1.093	0.880	0.602	0.539	0.530

Second circulation solution using regular hexagon

PSI	0.200	0.300	0.400	0.500	0.524
K/U	Gin/Yf	Gin/Yf	Gin/Yf	Gin/Yf	Gin/Yf
0.10	0.569	0.375	0.276	0.216	0.205
0.15	0.853	0.561	0.413	0.323	0.306
0.20	1.133	0.744	0.546	0.426	0.404
0.25	1.407	0.921	0.674	0.524	0.496
0.30	1.661	1.082	0.786	0.604	0.571
0.35	1.915	1.241	0.897	0.685	0.646
0.40	2.155	1.388	0.997	0.758	0.713
0.45	2.375	1.516	1.083	0.820	0.771
0.50	2.583	1.619	1.151	0.871	0.818
0.55	-0.000	1.693	1.199	0.910	0.856
0.60	3.079	1.739	1.229	0.938	0.884
0.65	2.881	1.759	1.245	0.957	0.903
0.70	2.739	1.753	1.248	0.968	0.915
0.75	2.462	1.720	1.231	0.955	0.910
0.80	2.374	1.648	1.239	0.961	0.915
0.85	2.350	1.617	1.237	0.964	0.918
0.90	2.314	1.623	1.223	0.960	0.916
0.95	2.018	1.577	1.237	0.962	0.914

where f is the operating frequency and f_0 is the center frequency. The ferrite material is assumed to be just saturated and the value of κ/μ is given by

$$\frac{\kappa}{\mu} = \frac{\gamma M_0}{\omega \mu_0}. \tag{40}$$

γ is the gyromagnetic ratio (2.21×10^5(rad/s/(A/m)), μ_0 the permeability of free space ($4\pi \times 10^{-7}$ H/m), and M_0 the saturation magnetization (Telsa).

One interesting case is the class of devices which are arranged so that κ/μ is 0.67 at the center of frequency. This implies that the value of κ/μ varies from 0.5 to 1.0 over an octave frequency band. The input admittance of a junction using a disk resonator is shown in Fig. 10 for a range of coupling angles ψ between 0.45 and 0.8. For smaller coupling angles, the equivalent circuit is not well behaved over the frequency interval. The input admittance is, in general, complex except for ψ close to 0.5 where it is a nearly frequency independent conductance. This is the so-called tracking solution [5], [16].

In Fig. 11, the frequency response of a circulator using the triangular resonator is given. While G/Y_f is nearly

TABLE V
TABLES OF $k_{eff}R$ (TABLE A) AND G/Y_f) TABLE B) FOR CIRCULATORS USING DISK, TRIANGLE, REGULAR HEXAGON, NARROW AND BROAD-WALL COUPLED IRREGULAR HEXAGON ($\phi = 50$), RESPECTIVELY

First circulation solution using irregular hexagon narrow wall coupled ($\phi = 50$)

PSI	0.200	0.300	0.400	0.436
K/U	Keff.R	Keff.R	Keff.R	Keff.R
0.10	2.004	2.003	2.002	2.002
0.15	1.997	1.995	1.993	1.992
0.20	1.988	1.985	1.980	1.978
0.25	1.976	1.971	1.964	1.961
0.30	1.953	1.955	1.944	1.939
0.35	1.949	1.937	1.920	1.912
0.40	1.934	1.916	1.891	1.881
0.45	1.919	1.892	1.857	1.843
0.50	1.903	1.862	1.815	1.797
0.55	1.893	1.823	1.761	1.738
0.60	2.542	1.778	1.697	1.670
0.65	2.505	1.731	1.622	1.592
0.70	2.441	1.617	1.523	1.499
0.75	2.556	2.084	1.365	1.347
0.80	2.564	1.854	1.256	1.217
0.85	2.570	1.633	1.122	1.073
0.90	1.856	1.372	0.933	0.892
0.95	1.173	0.999	0.671	0.635

Second circulation solution using irregular hexagon narrow wall coupled ($\phi = 50$)

PSI	0.200	0.300	0.400	0.436
K/U	Gin/Yf	Gin/Yf	Gin/Yf	Gin/Yf
0.10	0.424	0.280	0.207	0.188
0.15	0.635	0.418	0.308	0.281
0.20	0.844	0.555	0.408	0.371
0.25	1.050	0.689	0.505	0.459
0.30	1.252	0.819	0.598	0.542
0.35	1.449	0.944	0.686	0.621
0.40	1.639	1.063	0.769	0.695
0.45	1.815	1.172	0.844	0.761
0.50	1.972	1.263	0.906	0.816
0.55	2.117	1.331	0.951	0.857
0.60	2.683	1.385	0.984	0.888
0.65	2.463	1.428	1.010	0.912
0.70	2.357	1.439	1.025	0.929
0.75	0.036	1.363	1.024	0.931
0.80	-0.547	1.308	1.035	0.936
0.85	-0.141	1.276	1.039	0.939
0.90	1.524	1.245	1.035	0.937
0.95	1.460	1.181	1.032	0.935

TABLE VI
TABLES OF $k_{eff}R$ (TABLE A) AND G/Y_f (TABLE B) FOR CIRCULATORS USING DISK, TRIANGLE, REGULAR HEXAGON, NARROW AND BROAD-WALL COUPLED IRREGULAR HEXAGON ($\phi = 50$), RESPECTIVELY

First circulation solution using irregular hexagon broad wall coupled ($\phi = 50$)

PSI	0.200	0.300	0.400	0.500	0.600	0.611
K/U	Keff.R	Keff.R	Keff.R	Keff.R	Keff.R	Keff.R
0.10	2.004	2.002	2.000	1.997	1.994	1.912
0.15	1.997	1.993	1.988	1.981	1.974	1.857
0.20	1.986	1.979	1.970	1.958	1.945	1.802
0.25	1.973	1.961	1.945	1.926	1.906	1.747
0.30	1.958	1.939	1.914	1.885	1.857	1.691
0.35	1.942	1.912	1.875	1.835	1.799	1.633
0.40	1.928	1.880	1.827	1.776	1.731	1.573
0.45	1.926	1.844	1.771	1.707	1.656	1.510
0.50	2.273	1.805	1.707	1.630	1.572	1.444
0.55	2.251	1.764	1.632	1.544	1.481	1.374
0.60	2.185	1.715	1.549	1.453	1.386	1.299
0.65	2.089	2.011	1.459	1.358	1.289	1.220
0.70	1.977	1.884	1.371	1.258	1.185	1.133
0.75	1.857	1.752	1.243	1.133	1.072	1.038
0.80	1.687	1.524	1.107	1.014	0.957	0.932
0.85	1.493	1.289	0.969	0.884	0.828	0.811
0.90	1.246	0.902	0.789	0.726	0.679	0.665
0.95	0.914	0.670	0.561	0.511	0.478	0.472

Second circulation solution using irregular hexagon broad wall coupled ($\phi = 50$)

PSI	0.200	0.300	0.400	0.500	0.600	0.611
K/U	Gin/Yf	Gin/Yf	Gin/Yf	Gin/Yf	Gin/Yf	Gin/Yf
0.10	0.719	0.473	0.348	0.271	0.219	0.414
0.15	1.075	0.706	0.518	0.403	0.324	0.467
0.20	1.425	0.934	0.683	0.529	0.424	0.493
0.25	1.768	1.154	0.841	0.648	0.516	0.505
0.30	2.099	1.364	0.987	0.755	0.597	0.509
0.35	2.416	1.558	1.119	0.850	0.667	0.509
0.40	2.720	1.733	1.234	0.931	0.726	0.507
0.45	3.022	1.886	1.329	0.999	0.777	0.503
0.50	3.875	2.014	1.406	1.057	0.822	0.498
0.55	3.760	2.116	1.461	1.103	0.861	0.492
0.60	3.563	2.163	1.482	1.126	0.886	0.485
0.65	3.327	2.278	1.479	1.131	0.898	0.477
0.70	3.079	2.128	1.479	1.130	0.901	0.468
0.75	2.870	2.026	1.445	1.101	0.893	0.461
0.80	2.832	2.023	1.413	1.094	0.899	0.452
0.85	2.781	1.994	1.396	1.090	0.901	0.444
0.90	2.776	1.921	1.369	1.077	0.897	0.437
0.95	2.680	1.950	1.400	1.092	0.893	0.426

frequency independent within specific limits, B/Y_f retains a finite slope over the whole range of coupling angles.

The result for a regular hexagon is given in Fig. 12. The smaller values of coupling, while exhibiting a small value of B/Y_f over the frequency range, cannot be described by a constant conductance. Conversely, devices with larger coupling angles, which exhibit a frequency independent G/Y_f, have a finite susceptance slope parameter. It can be seen that the solution remains well behaved for narrower coupling angles than the disk and triangle. An upper bound is placed on the maximum coupling angle which may be used by the width of the side of the hexagon to which the coupling port is connected.

It is also possible to design circulators using irregular hexagonal resonators which may be coupled through both the broad and narrow walls. The width of the narrow wall restricts the range of possible coupling angles to lower upper limit than that for the broad wall. The results for a narrow wall coupled circulator are given in Fig. 13 and for a broad-wall coupled device in Fig. 14. It is observed that

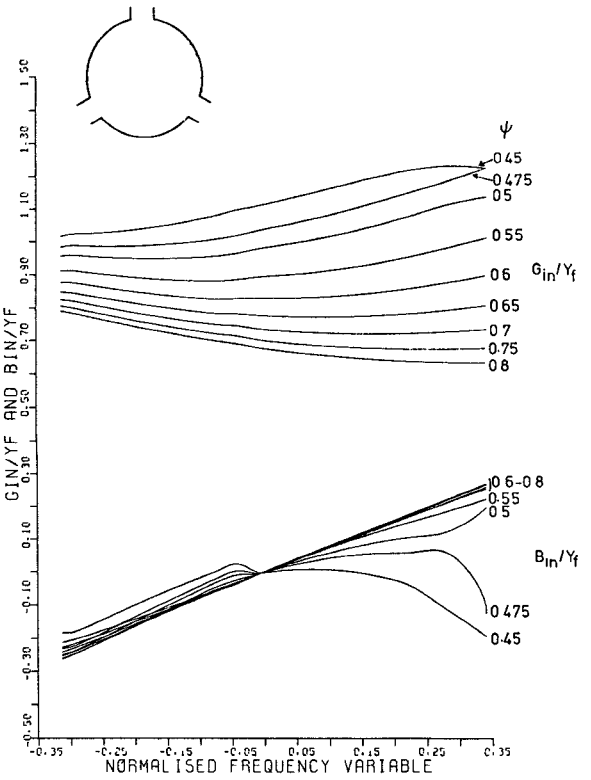

Fig. 10. Frequency response of planar circulator using disk resonator ($\kappa/\mu = 0.67$).

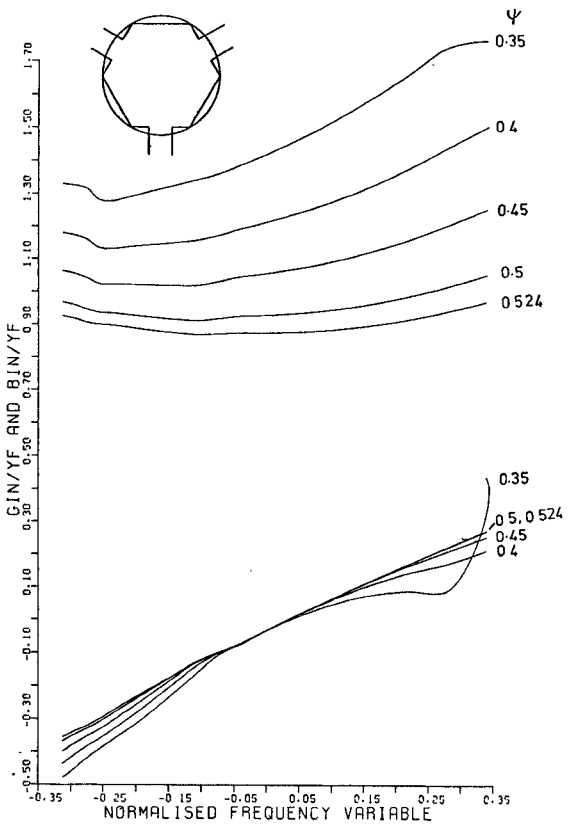

Fig. 12. Frequency response of planar circulator using regular hexagonal resonator ($\kappa/\mu = 0.67$).

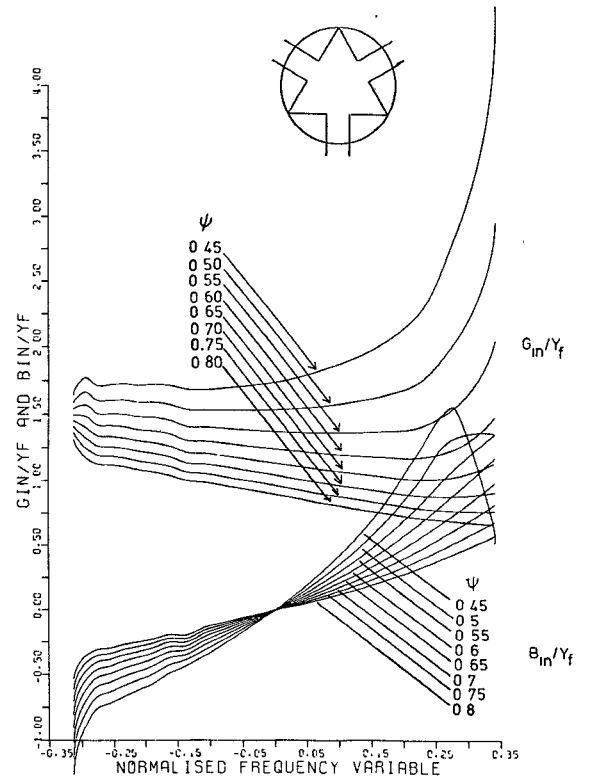

Fig. 11. Frequency response of planar circulator using triangular resonator ($\kappa/\mu = 0.67$).

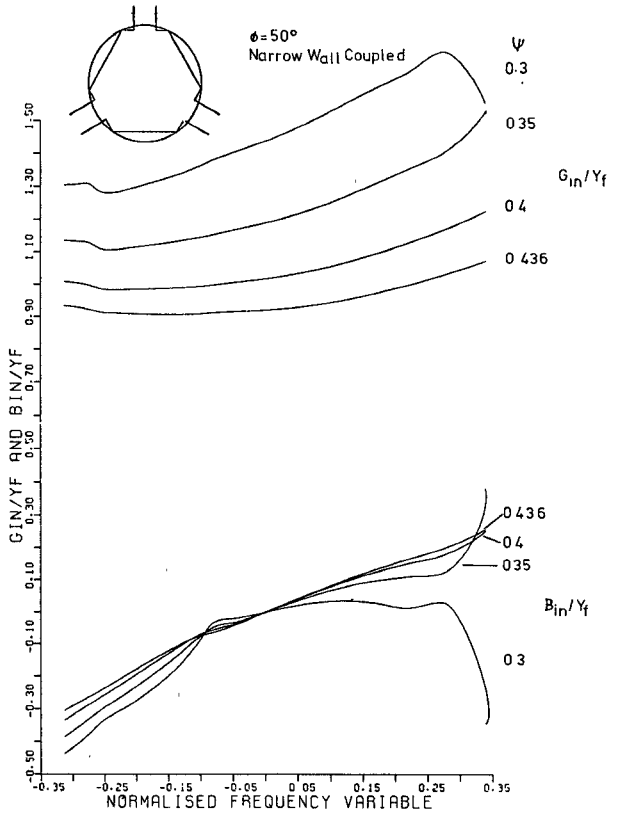

Fig. 13. Frequency response of planar circulator using irregular hexagonal resonator ($\kappa/\mu = 0.67$).

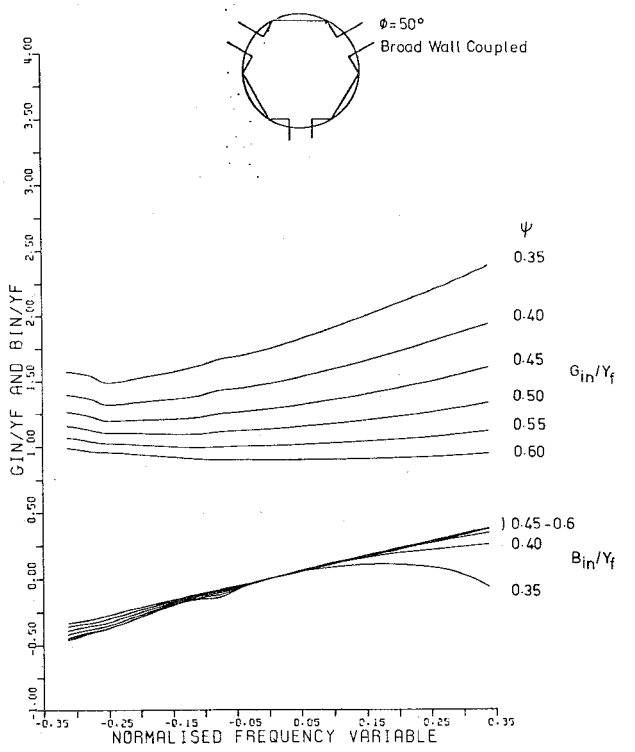

Fig. 14. Frequency response of planar circulator using irregular hexagonal resonator ($\kappa/\mu = 0.67$).

the gyrator conductance of disk, regular and irregular hexagons by and large exhibit the same values for the optimum coupling angle in the tracking region.

VII. Conclusions

This paper has described a finite element analysis of planar junction circulators. It has been used to calculate the circulation conditions of devices using disk, triangular, regular, and irregular hexagons over the range $0 < \kappa/\mu < 1$.

The method can also be used to plot the frequency response of junctions. In order to demonstrate this, the octave band defined by the so-called tracking interval, $0.5 < \kappa/\mu < 1.0$, has been studied for each of the resonators discussed previously.

Acknowledgment

The authors would like to thank the Procurement Executive, Ministry of Defense, (DCVD, UK) who sponsored this work.

References

[1] H. Bosma, "On stripline circulation at UHF," *IEEE Trans. Microwave Theory Tech.*, (1963 Symp. Issue), vol. MTT-12, pp. 61–72, Jan. 1964.
[2] H. Bosma, "Junction Circulators," *Advances in Microwaves*, vol. 6, pp. 215–239, 1971.
[3] J. B. Davies and P. Cohen, "Theoretical design of symmetrical junction circulator," *IEEE Trans. Microwave Theory Tech.*, vol. MTT-11, pp. 506–512, Nov. 1963.
[4] C. E. Fay and R. L. Comstock, "Operation of the ferrite junction circulator," *IEEE Trans. Microwave Theory Tech.*, vol. MTT-13, pp. 15–27, Jan. 1965.
[5] Y. S. Wu and F. J. Rosenbaum, "Wideband operation of microstrip circulators," *IEEE Trans. Microwave Theory Tech.*, vol. MTT-22, pp. 849–856, Oct. 1974.
[6] J. Helszajn, D. S. James, and W. T. Nisbet, "Circulators using planar triangular resonators," *IEEE Trans. Microwave Theory Tech.*, vol. MTT-27, pp. 188–193, Feb. 1979.
[7] J. Helszajn and W. T. Nisbet, "Circulators using planar wye resonators," *IEEE Trans. Microwave Theory Tech.*, vol. MTT-29, pp. 689–699, July 1981.
[8] T. Miyoshi, S. Yamaguchi, and S. Goto, "Ferrite planar circuits in microwave integrated circuits," *IEEE Trans. Microwave Theory Tech.*, vol. MTT-25, pp. 593–600, July 1977.
[9] T. Miyoshi and S. Miyaushi, "The design of planar circulators for wideband operation," *IEEE Trans. Microwave Theory Tech.*, vol. MTT-28, pp. 210–215, Mar. 1980.
[10] P. Silvester, "Finite element solution of the homogeneous waveguide problem," *Alta Frequenza*, vol. 38, pp. 593–600, May 1969.
[11] P. Silvester, "High order polynomial triangular finite elements for potential problem," *Int. J. Eng. Sci.*, vol. 7, pp. 849–861, 1969.
[12] P. Silvester, "A general high-order finite element waveguide analysis program," *IEEE Trans. Microwave Theory Tech.*, vol. MTT-17, pp. 204–210, Apr. 1969.
[13] Z. J. Csendes and P. Silvester, "Numerical solution of dielectric-loaded waveguides—Part 1: "Finite element analysis," *IEEE Trans. Microwave Theory Tech.*, vol. MTT-18, pp. 1124–1131, Dec. 1970.
[14] Z. J. Csendes and P. Silvester, "Numerical solution of dielectric-loaded waveguides—Part 2: "Modal approximation technique," *IEEE Trans. Microwave Theory Tech.*, vol. MTT-19, pp. 504–509, June 1971.
[15] J. K. Richardson, "An approximate method of calculating Z_0 of a symmetric stripline," *IEEE Trans. Microwave Theory Tech.*, vol. MTT-15, pp. 130–131, 1967.
[16] J. Helszajn, "Operation of the tracking circulator," *IEEE Trans. Microwave Theory Tech.*, vol. MTT-29, pp. 700–707, July 1981.
[17] H. A. Wheeler, "Transmission line properties of parallel strips separated by a dielectric sheet," *IEEE Trans. Microwave Theory Tech.*, vol. MTT-13, pp. 172–185 Mar. 1965.
[18] W. T. Nisbet and J. Helszajn, "Mode charts for microstrip resonators on dielectric and magnetic substrates using a transverse resonance method," *Microwave, Opt., Acoust.*, vol. 3, no. 2, pp. 69–77, Mar. 1979.

Ronald W. Lyon (M'76) was born in Edinburgh, Scotland, on September 4, 1953. He received the B.Sc. and Ph.D. degrees from Heriot–Watt University, Edinburgh, in 1975 and 1979, respectively.

From 1975 until 1978 he was employed at Heriot–Watt University investigating slotted waveguide. Subsequently, from 1978 unitl 1981, he was involved in post-doctoral research into planar circulators, also at Heriot–Watt. He is now a Senior Research Engineer working on planar array antennas with the RF Technology Centre, ERA Technology Ltd., Leatherhead, England.

Dr. Lyon is an Associate Member of the Institution of Electrical Engineers, London.

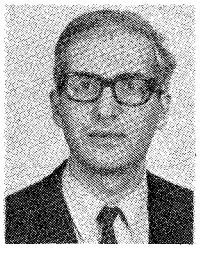

Joseph Helszajn (M'64) was born in Brussels, Belgium, in 1934. He received the Full Technological Certificate of the City and Guilds of London Institute from Northern Polytechnic, London, England in 1955, the M.S.E.E. degree from the University of Santa Clara, Santa Clara, CA, in 1964, the Ph.D. degree from the University of Leeds, Leeds, England, in 1969, and the D.Sc. degree from Heriot-Watt University, Edinburgh, Scotland, in 1976.

He has held a number of positions in the microwave industry. From 1964 to 1966 he was Product Line Manager at Microwave Associates, Inc., Burlington, MA. He is a consultant to several microwave companies and is a Reader at Heriot-Watt University. He is the author of the books *Principles of Microwave Ferrite Engineering* (New York: Wiley, 1969), *Nonreciprocal Microwave Junctions and Circulators* (New York: Wiley, 1975), and *Passive and Active Microwave Circuits* (New York: Wiley, 1978).

Dr. Helszajn is a Fellow of the Institution of Electronic and Radio Engineers (England), and a Fellow of the Institution of Electrical Engineers. In 1968, he was awarded the Insignia Award of the City of Guilds of London Institute. He is an Honorary Editor of *Microwaves, Optics, and Antennas* (I.E.E. Proceedings).